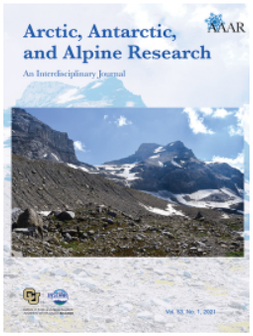

Taylor & Francis
Taylor & Francis Group

Arctic, Antarctic, and Alpine Research
An Interdisciplinary Journal

ISSN: (Print) (Online) Journal homepage: https://www.tandfonline.com/loi/uaar20

Physical, chemical, and biological characteristics of supraglacial pools on a debris-covered glacier in Mt. Gongga, Tibetan Plateau

Heather Fair, Peter C. Smiley Jr. & Liu Qiao

To cite this article: Heather Fair, Peter C. Smiley Jr. & Liu Qiao (2020) Physical, chemical, and biological characteristics of supraglacial pools on a debris-covered glacier in Mt. Gongga, Tibetan Plateau, Arctic, Antarctic, and Alpine Research, 52:1, 635-649, DOI: 10.1080/15230430.2020.1839165

To link to this article: https://doi.org/10.1080/15230430.2020.1839165

ARCTIC, ANTARCTIC, AND ALPINE RESEARCH
2020, VOL. 52, NO. 1, 635–649
https://doi.org/10.1080/15230430.2020.1839165

Taylor & Francis
Taylor & Francis Group

Physical, chemical, and biological characteristics of supraglacial pools on a debris-covered glacier in Mt. Gongga, Tibetan Plateau

Heather Fair[a], Peter C. Smiley Jr.[b], and Liu Qiao[c]

[a]Department of Biology, Kenyon College, Gambier, Ohio, USA; [b]Soil Drainage Research Unit, USDA Agricultural Research Service, Columbus, Ohio, USA; [c]Institute of Mountain Hazards and Environment, Chinese Academy of Sciences, Chengdu, China

ABSTRACT

Meltwater habitats are found on glacier surfaces worldwide, but much of the current understanding of these habitats comes from clean glaciers sprinkled with cryoconite. Cryoconite is windblown dust particles covered with biological material that form small meltwater holes due to difference in the albedo of cryoconite compared to clean ice. However, no information is available on the physical, chemical, and biological characteristics of supraglacial pools on debris-covered glaciers. We measured physical and chemical variables and sampled macroinvertebrates from forty-six supraglacial pools during the summers of 2018 and 2019 on the debris-covered Hailuogou Glacier in southeastern Tibet. Our physical and chemical results indicated that the sampled supraglacial pools exhibited a greater diversity of shapes, were larger, contained larger substrate sizes, and had greater substrate diversity than cryoconite holes. The sampled supraglacial pools frequently contained Chironomidae (Diptera) and Isotomidae (Collembola), which are macroinvertebrate taxa that are uncommon in cryoconite holes. Chironomidae occurrence and abundance was not correlated with any measured environmental variable. The best predictors of Isotomidae and macroinvertebrate occurrence and abundance were conductivity, ice to water surface depth, and number of supraglacial pools within 5 m. Our results highlight the uniqueness of supraglacial pools on a debris-covered glacier in southeastern Tibet.

ARTICLE HISTORY
Received 12 June 2020
Revised 7 October 2020
Accepted 15 October 2020

KEYWORDS
Debris-covered glacier; macroinvertebrates; macroinvertebrate–habitat relationships; Isotomidae; conductivity

Introduction

Glacier surfaces are complex environments containing a variety of aquatic habitats created by the melting of glacier ice. Examples of supraglacial aquatic habitats include cryoconite holes, pools, lakes, and supraglacial streams. Among these glacial meltwater habitat types much of the current understanding comes from cryoconite holes found on clean surface glaciers. Cryoconite holes are formed when sand moves onto clean ice (blue or white ice) via eolian transport, avalanches, or landslides. Microbial organisms form layers around the sand, which has a lower albedo than ice, leading to the formation of meltwater-filled depressions with dark mud-like substrate (Adams 1966; Wharton et al. 1985; Takeuchi et al. 2000; Zawierucha et al. 2018). Cryoconite sediments contain microbial organisms, including bacteria, cyanobacteria, and algae (Takeuchi et al. 2000; Mueller et al. 2001; Tranter et al. 2004; Hodson et al. 2008) and are mixed with organic and detrital material (Mueller et al. 2001; Tranter et al. 2004). The thickness of sediment at the bottom of cryoconite holes ranges from 0.4 to 2.5 cm in Greenland (Cook et al. 2010), Nepal (Takeuchi et al. 2000), and Antarctica (Telling et al. 2014). Cryoconite holes can occupy up to 10 percent of glacier ablation surfaces (Hodson et al. 2008; Cook et al. 2010; Edwards et al. 2011).

Information on the physical characteristics and water chemistry of cryoconite holes has been reported from ice sheets and glaciers in Antarctica, Svalbard, Greenland, Italy, Canada, and Asia (Table 1). The diameter of cryoconite holes is one of the most frequently measured physical variables and ranges from 0.01 m to 5 m (Bagshaw et al. 2011; Table 1). Other less commonly measured physical variables include area and water depth measurements (Table 1). Chemical variables commonly measured in cryoconite holes include pH, conductivity, and water temperature (Table 1).

Cryoconite holes are known hotspots for microbial diversity and metabolic activity (Margesin and Miteva

CONTACT Heather Fair hebfair@yahoo.com Department of Biology, Kenyon College, 108 Higley Hall, Gambier, OH 43022, USA.
Supplemental data for this article can be accessed on the publisher's website.

Table 1. Summary of the means (Mn), ranges (Rg), and single values (Sv) of the diameter, surface area, water depth, pH, electrical conductivity, and water temperature of cryoconite holes from glaciers and ice sheets in Svalbard, Greenland, Canada, Italy, Nepal, and Antarctica.

Location	Diameter (cm)	Surface area (cm^2)	Water depth (cm)	pH	Electrical conductivity (µS/cm)	Water temperature (°C)
Svalbard[a]	Rg: 8.0–12.0	—	—	Sv: 4.6	Sv: 38	Sv: 0.2
Svalbard[b]	—	—	Rg: 0.1–49.0	—	—	—
Svalbard[c]	—	—	—	Mn: 6.9 Rg: 6.5–7.5	Mn: 21 Rg: 5–53	—
Svalbard[d]	—	Mn: 1,287 Rg: 56–31949	Mn: 10.8 Rg: 0.5–27.1	—	—	—
Svalbard[e]	—	—	Mn: 5.6 Rg: 3.5–9.0	Mn: 7.9 Rg: 5.8–9.4	Mn: 40 Rg: 7–86	Rg: 0.05–0.22
Greenland[f]	Mn: 5.0–7.0	—	Mn: 7.4 Rg: 1.0–16.0	Mn: 5.8 Rg: 4.9–8.2	—	—
Greenland[g]	—	Rg: 3–1559	—	—	—	—
Canada[h]	Mn: 2.3 Rg: 1.3–4.3	—	—	—	—	—
Canada[i]	—	—	—	—	—	Rg: −1.0 to 2.0
Canada[j]	Mn: 27.1	Mn: 639	—	Mn: 3.9	Mn: 11	—
Italy[k]	Mn: 19.4	—	Mn: 8.4	Mn: 6.2	Mn: 7	—
Nepal[l]	Mn: 7.0 Rg: 1.0–36.0	—	Mn: 1.9 Rg: 0.1–6.1	—	—	—
Antarctica[j]	Mn: 38.7	Mn: 1,677	—	Mn: 7.9	Mn: 27	—
Antarctica[m]	Mn: 22.0–38.0	—	—	Mn: 5.8–8.10	Mn: 60–125	—
Antarctica[n]	—	Mn: 777 Rg: 154–4185	—	Mn: 7.0 Rg: 6–10	Mn: 34 Rg: 5–73	—
Antarctica[o]	—	Rg: 257.0–729.0	—	—	—	—
Antarctica[p]	Rg: 20.0–120.0	—	Rg: 30.0–40.0	Mn: 9.6	—	—
Antarctica[q]	—	—	—	—	Rg: 5–21	Rg: −9 to 1.8
Antarctica[r]	Mn: 25.8–47.3	—	Mn: 0.0–12.1	Mn: 8.9	—	—
King George Island[s]	Mn: 10.0	—	Mn: 15.6	—	—	—

Sources. [a]De Smet and Van Rompu (1994). [b]Vonnahme et al. (2016). [c]Zawierucha, Ostrowska et al. (2016). [d]Zawierucha, Vonnahme et al. (2016). [e]Zawierucha, Buda, and Nawrot (2019). [f]Zawierucha et al. (2018). [g]Cook et al. (2018). [h]Adams (1966). [i]McIntyre (1984). [j]Mueller et al. (2001). [k]Zawierucha, Buda, Azzoni et al. (2019). [l]Takeuchi et al. (2000). [m]Porazinska et al. (2004). [n]Sommers et al. (2018). [o]Darcy et al. (2018). [p]Tranter et al. (2004). [q]Bagshaw et al. (2011). [r]Telling et al. (2014). [s]Buda et al. (2020).

2011) despite water temperatures frequently below 2°C. Cryoconite holes host communities of microbes, autotrophic microorganisms, and invertebrates of a range of sizes (Zawierucha et al. 2015; Pittino et al. 2018), but the main focus of cryoconite hole research involving the biota has been on microbial diversity. Zawierucha et al. (2015) compiled a global list of invertebrates found within cryoconite holes that confirmed the occurrence of meiofauna taxa Rotifera, Tardigrada, Nematoda, Copepoda and macroinvertebrate taxa Chironomidae, Plecoptera, and Collembola. These natural history surveys confirm that invertebrates are a component of the aquatic communities within cryoconite holes. The few studies that have quantified invertebrate habitat relationships have focused on Rotifera (rotifers) and Tardigrada (water bears) in cryoconite holes in Svalbard, Greenland, and King George Island (Vonnahme et al. 2016; Zawierucha, Vonnahme et al. 2016; Zawieruch et al. 2018; Zawierucha, Budy, Fontaneto et al. 2019; Zawierucha, Buda, and Nawrot 2019; Buda et al. 2020). However, more information on invertebrate–habitat relationships is needed to fully understand the abiotic and biotic factors influencing the biodiversity within cryoconite holes and other glacial meltwater habitats.

Glacial meltwater habitats and their biodiversity have not been studied on debris-covered glaciers, which are becoming more prevalent worldwide because of climate warming, which causes glacier ablation and intensified paraglacial rock falls (Caccianiga et al. 2011). Debris-covered glaciers are ubiquitous in the Himalayas, with 80 percent of valley glaciers having ablation zones that are covered with supraglacial debris (Fujii and Higuchi 1977). In southeastern Tibet's Three Parallel Rivers region (Yangtze, Mekong, and Salween) where climate-induced melting is severe (He et al. 2008; Yao et al. 2012), vertical relief is prominent and glacier ablation zones extend well below the tree line (Baker and Moseley 2007). Here, avalanches and debris flows frequently contribute to the debris layers, which can be over a meter thick on the lowest elevations of glaciers (Zhang et al. 2011). A line of demarcation on ablation zones of debris-covered glaciers delineates the transition from thin debris coverage where melt rates are higher to thicker debris coverage located near the terminus where melt rates are lower (Fyffe et al. 2019).

Preliminary fieldwork on the debris-covered Hailuogou Glacier in Tibet resulted in observations of supraglacial pools that appear similar to cryoconite holes in that they are small lentic meltwater habitats found on the glacier surface. Our observations also indicated that supraglacial pools might contain larger sediment sizes than cryoconite holes found on clean

glaciers that contain cryoconite, which is typically less than 3 mm in diameter (Takeuchi et al. 2000; Cook et al. 2010). Supraglacial pools on debris-covered glaciers are likely formed by a mechanism similar to that of cryoconite holes, but the process may be further influenced by debris heating, stippled glacier surfaces, debris size, debris position relative to the hole, and differential debris coverage that influences where supraglacial pools form. Cryoconite and the small cryoconite holes they form have a tremendous impact on the melt processes and ecology of clean glaciers (Adams 1966). However, the impact of supraglacial debris on the formation of supraglacial pools and on the melt processes of debris-covered glaciers is largely unknown.

Our objective was to document the physical characteristics, chemical characteristics, and aquatic macroinvertebrates within supraglacial pools on the debris-covered Hailuogou Glacier on Mt. Gongga in southeastern Tibet. Additionally, we aimed to identify the best predictors of macroinvertebrate abundance and occurrence in the supraglacial pools on this glacier. Our research questions were the following:

(1) What are the physical habitat and chemical characteristics of supraglacial pools on a debris-covered glacier?
(2) What macroinvertebrates occur within supraglacial pools on a debris-covered glacier?
(3) What physical habitat and chemical variables best predict macroinvertebrate abundance and occurrence within these supraglacial pools?

To address these questions, we measured physical and chemical variables and sampled macroinvertebrates from forty-six supraglacial pools during the summer monsoon seasons of 2018 and 2019 on the debris-covered Hailuogou Glacier. To our knowledge, this is the first documentation of the physical and chemical conditions of supraglacial pools on a debris-covered glacier and of the macroinvertebrate–habitat relationships within supraglacial pools on a debris-covered glacier.

Methods

Study area

Our study was conducted on the Hailuogou Glacier, a monsoon temperate glacier with a debris-covered tongue terminating at 2,990 m a.s.l. in the Hailuogou valley located on the eastern slope of Mt. Gongga in the Daxueshan mountain range, southeastern Tibet (Figure 1). Mt. Gongga is located on the southeastern margin of the Tibetan Plateau, where the climate is dominated by the East Asian monsoon during the summer. Climatic observations from the Gongga Station (3,000 m a.s.l.; Figure 1) indicate that the mean annual air temperature is 4.1°C and mean annual precipitation is 1,900 mm (Liu et al. 2010). Air temperature in the region increased 0.13°C per decade between 1952 and 2009 (Liu et al. 2010). There are seventy-four monsoonal temperate glaciers distributed around the Daxueshan mountain range, and most are debris-covered (Figure 1).

The Hailuogou Glacier extends about 13 km in length and 24.7 km^2 in area, with altitudes ranging from 2,990 to 7,556 m a.s.l. It has a wide cirque accumulation zone (7,556–4,980 m a.s.l.) and a 1,080-m-high ice fall (4,780–3,700 m a.s.l.) below the accumulation zone and approximately 1 km west of our upper sampling sites. The sampled lower ice tongue (Figure 1) has experienced continuous and remarkable shrinkage during the past forty years, with the terminus retreating by about 2 km since 1930 and ice thinning at a rate of 1.1 m a^{-1} between 1966 and 2009 (Liu et al. 2010). The lower part of the ice tongue is covered by a debris layer that increases in thickness down-glacier and reaches about 1.5 m thick near the terminus (Zhang et al. 2011). During the early ablation season (April to early May), supraglacial lakes or water ponded by crevasses can be found in the region of relative flat ice surfaces between 3,500 and 3,600 m a.s.l. (Liu and Liu 2010).

In 2018 and 2019 we attempted to stratify our sampling efforts so that approximately one half of the supraglacial pools sampled were located on the upper ablation tongue above the heavy debris-covered zone (debris thickness 1–20 cm) and one half of the supraglacial pools were located on the lower section of the ablation zone containing thicker layers of debris up to 1.5 m thick (Zhang et al. 2011). In 2018, twenty-one supraglacial pools were sampled on the upper ablation tongue on 3 June and 4 June, and seven supraglacial pools were sampled in the lower ablation zone on 30 May. In 2019, nine supraglacial pools were sampled on the upper ablation zone on 2 August and nine holes were sampled in the lower ablation zone on 3 August. We were not able to randomly select supraglacial pools to sample before sampling began because the pools are not visible on aerial images. We haphazardly selected supraglacial pools with meltwater as we encountered them and then searched for surrounding pools in a 20-m circular pattern around the sampled pool before moving on to the next pool. The accessibility of the surrounding terrain played a factor in our ability to locate pools to sample, especially in areas with deep crevasses. Debris depth in certain places on the lower ablation zone made it challenging to locate supraglacial pools. In 2019, the logistics of getting to the lower ablation

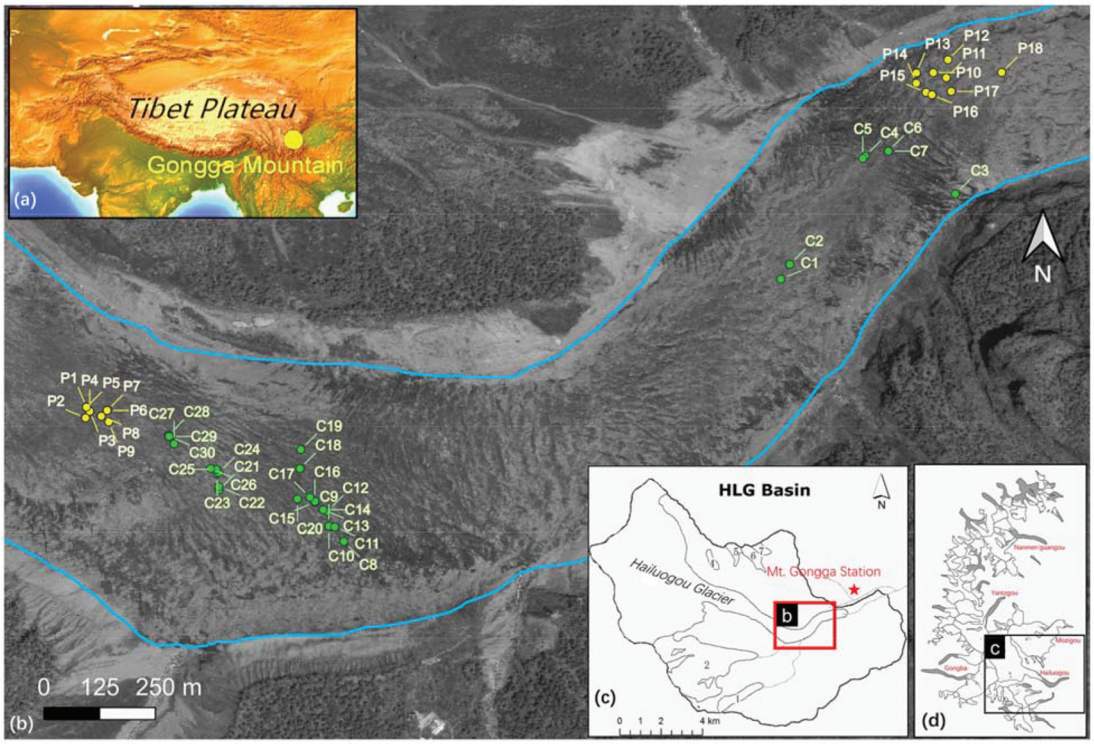

Figure 1. (a) Map showing location of Mount Gongga in Tibet, (b) Chinese Gaofen-2 aerial photograph (acquired on 14 May 2015) of Hailuogou Glacier depicting the location of the supraglacial pools sampled (green dots, pools sampled in 2018; yellow dots, pools sampled in 2019), (c) map of Hailuogou Glacier basin and the location of the Mt. Gongga station, (d) and glacier distribution in the Mt. Gongga range, with debris cover shown in gray.

zone to sample supraglacial pools was further complicated by a paraglacial landslide that damaged the staircase that provided access to the lower ablation zone.

We selected supraglacial pools containing meltwater to collect macroinvertebrates and measure physical and chemical variables. We did not sample for macroinvertebrates from two supraglacial pools we encountered with a diameter less than 5 cm due to either the absence of water or the inability to fit the sampling net into the pools. We considered supraglacial pools greater than 2.5 m diameter to represent a different habitat type that would not be comparable to cryoconite holes. We only encountered a few of these larger supraglacial meltwater habitats, and these were typically located at the base of large crevasses. Sampling these few smaller and larger meltwater habitats would have required using different sampling methods to capture macroinvertebrates that would have introduced sampling gear bias into our data. In 2019 we ensured that we did not repeatedly sample any supraglacial pool that was sampled in 2018 by searching within different areas of the upper and lower ablation zones and by comparing the Global Positioning System (GPS) coordinates of pools sampled in 2018 with those sampled in 2019.

Physical and chemical measurements

We measured the physical and chemical characteristics of each supraglacial pool before sampling for macroinvertebrates. The average of all (one to four) width and length measurements (LW) was used to calculate the surface area of each supraglacial pool. Mean LW for a rectangular or square-shaped supraglacial pool is analogous to the diameter of circular cryoconite holes. Four to six measurements of water depth and the distance from ice surface to the water surface were also obtained for each pool with a tape measure. Water velocity was measured only if there was a visible source of supraglacial flowing water into or within the pool. Preliminary water velocity measurements obtained with a Global Water FP101 flow probe (Gold River, CA) found that velocity readings were less than the detectable limit (0.1 m/s).

We visually estimated turbidity prior to any disturbance of the water. We did not have access to a turbidity meter, and using a turbidity tube would have required complete removal of all water from the smaller pools, which would have negatively impacted our macroinvertebrate sampling. We assigned the turbidity of each hole into one of four categories: (1) very clear (bottom substrate visible), (2) clear (bottom substrate visible but with slight haze in the water column), (3) turbid (water

a gray color and the bottom substrate is difficult to see), and (4) very turbid (water color is gray or brown and bottom substrate is not visible). In situ measurements of water temperature, conductivity, and pH were obtained in each supraglacial pool with a YSI Professional Plus (Yellow Springs, OH) multiparameter meter that was calibrated at the beginning of each sampling season.

We used a gravelometer to measure the size of 100 randomly selected substrate pieces from within each supraglacial pool and then calculated substrate richness as the number of fifteen substrate size categories found in each pool (2, 2.8, 4, 5.6, 8, 11, 16, 22.6, 32, 45, 64, 90, 128, >180 mm), mean grain size, and the percentage sand (<2 mm), gravel (2–64 mm), cobble (64–180 mm), and large cobble/boulders (>180 mm).

We used a handheld GPS to obtain the coordinates and elevation of each supraglacial pool and ArcMap (ESRI 2013) and the GPS coordinates to calculate seven glacier landscape variables. The calculated glacier landscape variables included (1) the distance from the sampled pool to the northern and southern boundaries of the glacier (i.e., the transition between the glacial moraine and terrestrial vegetation); (2) glacier width (sum of distances from the northern and southern boundaries of the glacier); (3) distance to the nearest terrestrial vegetation (the smallest distance of the distances of the northern and southern boundaries); (4) the difference in distances of northern and southern glacier boundaries; (5) the ratio of the distance to the nearest vegetation and glacier width; (6) distance to nearest sampled supraglacial pool; and (7) number of sampled supraglacial pools within 5 m. These seven glacier landscape variables were derived from island biogeography and edge effect concepts and described the distance of sampled pools from a source of macroinvertebrate colonists outside the glacier (distances from northern and southern boundaries, glacier width, distance to nearest vegetation), the relative location of the sampled pools with respect to the edge of the glacier (difference between northern and southern boundaries, ratio of distance to nearest vegetation and glacier width), or the distance of sampled pools from a local source of macroinvertebrate colonists on the glacier (distance to nearest pool and number of pools within 5 m).

Macroinvertebrate collection and identification

Macroinvertebrates were collected from supraglacial pools with a telescoping 20.3- or 30.5-cm triangular dipnet (mesh size 750–800 μm) depending on the diameter of the pool. The 20.3-cm dipnet was used in supraglacial pools with diameters less than 30 cm and the 30.5-cm dipnet was used in supraglacial pools with diameters greater than 35 cm. Four to five dipnet sweeps were made in each pool and we ensured that each dipnet sweep sampled macroinvertebrates from the bottom substrate, water column, and water surface. Captured macroinvertebrates were preserved in 99 percent ethanol in the field. Macroinvertebrates were separated from organic material in the laboratory and identified and enumerated in the laboratory using a dissecting microscope (7× to 40× magnification). All captured macroinvertebrates were identified to family level using taxonomic keys provided in Merritt et al. (2008).

Statistical analysis

We calculated the means and standard deviation of surface area, water depth, ice to water surface depth, number of supraglacial pools within 5 m, substrate richness, mean grain size, water temperature, conductivity, and pH to describe the physical and chemical characteristics of supraglacial pools. We used a *t*-test or Mann-Whitney test to determine whether selected physical and chemical characteristics differed between the upper and lower ablation zones. For those physical and chemical response variables that did not meet the assumptions of normality and equal variance, the Mann-Whitney test was used. We also calculated the mean and standard deviation of the abundance of each macroinvertebrate taxa captured. We used generalized linear model analysis to determine whether the abundance of each macroinvertebrate taxa differed between the upper and lower ablation zones.

Our analyses to determine the best predictors of macroinvertebrate abundance (number of animals captured) and occurrence within supraglacial pools consisted of a combination of generalized linear model analyses and Akaike's information criterion analyses. First, we selected thirteen predictors and conducted univariate generalized linear model analyses to identify which predictors significantly influenced our six response variables (Chironomidae abundance, Chironomidae occurrence, Isotomidae abundance, Isotomidae occurrence, macroinvertebrate abundance [sum of Chironomidae and Isotomidae abundance], and macroinvertebrate occurrence [occurrence of Chironomidae and/or Isotomidae]). Our thirteen predictors were (1) surface area, (2) mean water depth, (3) mean ice surface–to–water surface depth, (4) the difference in distance of northern and southern glacier boundaries, (5) distance to closest supraglacial pool, (6) number of supraglacial pools within 5 m, (7) ablation zone (upper or lower), (8) substrate richness, (9) mean grain size, (10) water temperature, (11) pH, (12) conductivity, and (13) turbidity. These thirteen environmental predictors were selected from among twenty-four environmental variables that we

calculated from our physical and chemical measurements. Eleven predictors were selected because preliminary Pearson correlation analyses indicated that they did not exhibit strong relationships (i.e., $r > 0.6$ or $r < -0.6$ and $p < .05$) with other predictors, which ensures that the multivariate models used in the second part of our analyses (see next paragraph for more details) are not influenced by multicollinearity, which can lead to spurious results. Two predictors (ablation zone and number of supraglacial pools within 5 m) were strongly correlated with each other ($r > 0.9$, $p < .05$) but were retained because we felt they might be important determinants of macroinvertebrate abundance and occurrence. Specifically, ablation zone was retained because it is a proxy for elevation and others have explored the influence of elevation on physical habitat variables and meiofauna in cryoconite holes (Gerdel and Drouet 1960; Takeuchi et al. 2018; Zawierucha et al. 2018). The number of supraglacial pools within 5 m was retained because it serves as an indicator of the number of available local sources of colonists immediately adjacent to the sampled pools.

The second step in determining the best predictors was to develop all possible univariate and multivariate generalized linear models with those predictor variables that we observed to have a significant effect ($p < .05$) on our six response variables in the initial univariate generalized linear model analyses. We then conducted multimodel inference analyses to identify which model best predicted the abundance and occurrence of Chironomidae, Isotomidae, and macroinvertebrates in supraglacial pools. Our multimodel inference analyses consisted of obtaining the small sample Akaike information criterion (AICc) score, ΔAICc (the difference in AICc between each model and the model with the minimum AICc), and the Akaike weight (*Wi*; Burnham and Anderson 2002; Johnson and Omland 2004). We also calculated percentage deviance [100 * (null deviance – residual deviance/null deviance)] of each model, which is an additional model diagnostic that indicates the amount of deviance accounted for in the model and is analogous to the well-known R^2 statistic (Guisan and Zimmermann 2000). We based our multimodel inference analysis on the AICc because the ratio of n/K was less than 40 for all models (Burnham and Anderson 2002; Johnson and Omland 2004). Multimodel inference analyses involving univariate and multivariate models were only conducted for Isotomidae abundance, macroinvertebrate abundance, and Isotomidae occurrence.

All statistical analyses were conducted with R (R Core Team 2017). *t*-Tests and Mann-Whitney tests were conducted with the t.test function in the stats package (R Core Team 2017). Pearson correlation analyses were conducted with the cor.test function from the stats package (R Core Team 2017). Generalized linear model analyses with abundance response variables were conducted with the negative binomial distribution using the glm.nb function from the MASS package (Venables and Ripley 2002). Generalized linear model analyses with occurrence response variables were conducted with the binomial distribution using the glm function within stats package (R Core Team 2017). AICc values were obtained with the AICc function within the AICcmodavg package (Mazerolle 2020).

Results

Physical and chemical characteristics

Mean LW of all Hailuogou Glacier supraglacial pools sampled was 49.8 cm (SD = 28.9) and the mean area was 3,539 cm^2 (SD = 6655). Mean water depth of Hailuogou Glacier supraglacial pools was 42 cm (SD = 57) and mean ice to water surface depth was 16 cm (SD = 20). Twenty-four percent of the pools contained water at the surface of the ice and 52 percent of the pools had mean ice to water surface depths of less than 10 cm. The mean number of supraglacial pools within 5 m was 0.5 (SD = 0.6). Mean grain size within the pools was 12.5 mm (SD = 8.2) and mean substrate richness was 10.0 (SD = 3.19), which reflected the heterogeneity of substrate sizes on debris-covered glaciers. Water temperatures within Hailuogou Glacier supraglacial pools ranged from supercooled (−0.01°C) to 4.5°C with an overall mean water temperature of 0.70°C (SD = 0.98). The mean conductivity was 20.78 μS/cm (SD = 14.03) and the pH of the water was 7.76 (SD = 0.70) in the supraglacial pools sampled. The only environmental variable that differed ($p < .05$) between the upper and lower ablation zones was the number of supraglacial pools within 5 m with the upper ablation zone having a greater number of supraglacial pools within 5 m than the lower ablation zone (Table 2).

Macroinvertebrates

We documented two macroinvertebrate families from forty-six captures during our two-year study. All specimens captured were either larval Chironomidae (Diptera, midges) or Isotomidae (Collembola, springtails). During sampling we noted Isotomidae on the surface of the water. Eighteen of the forty-six supraglacial pools contained Chironomidae, twenty-three of the forty-six supraglacial pools contained Isotomidae, and nine pools contained both taxa. The mean Chironomidae abundance of all Hailuogou Glacier supraglacial pools was 0.8 (SD = 1.6) and the mean Isotomidae abundance was 4.4 (SD = 12.5). Chironomidae abundance did not differ between the

Table 2. Mean (SD) of selected environmental variables and macroinvertebrate families in forty-six supraglacial pools within the upper and lower ablation zones on the Hailuogou Glacier in Ganze Tibetan Autonomous Region, China, June 2018 and August 2019.

	Upper ablation zone	Lower ablation zone
Environmental variables		
Mean LW (cm)	52.92(31.96)a	43.66(21.20)a
Area (cm^2)	4200 (8000)a	2500 (2500)a
Mean water depth (m)	0.47 (0.66)a	0.31 (0.29)a
Mean surface ice to water surface depth (m)	0.20 (0.23)a	0.08 (0.08)a
Number of cryoconite holes within 5 m	0.61 (0.67)a	0.13 (0.35)b
Mean grain size (mm)	11.51 (6.99)a	14.63 (10.20)a
Substrate richness	10.06 (3.18)a	9.93 (3.33)a
Water temperature (°C)	0.80 (1.07)a	0.49 (0.76)a
Conductivity (μS/cm)	21.10 (14.91)a	20.13 (12.50)a
pH	7.86 (0.37)a	7.56 (1.11)a
Macroinvertebrate families		
Isotomidae abundance	5.84 (14.97)a	1.53 (2.45)b
Chironomidae abundance	0.55 (0.93)a	1.40 (2.44)a

Note. Different letters within the rows indicate significant differences ($p < .05$) between the upper and lower ablation zones.

upper and lower ablation zones (Table 2). Isotomidae abundance was greater ($p < .05$) in the upper ablation zone than in the lower ablation zone (Table 2).

Evaluation of the best predictors

Chironomidae abundance was not influenced significantly ($p > .05$) by any of the thirteen environmental variables (Table 3). Isotomidae abundance exhibited a negative relationship with water temperature, conductivity, and ablation zone and a positive relationship with ice to water surface depth and number of supraglacial pools within 5 m (Table 3). Macroinvertebrate abundance was negatively correlated with conductivity and positively correlated with number of pools within 5 m and ice to water surface depth (Table 3). Chironomidae occurrence was not significantly correlated ($p > .05$) with any of the measured environmental variables (Table 3). Isotomidae occurrence was negatively correlated with conductivity and positively correlated with mean water depth (Table 3). Macroinvertebrate occurrence was negatively correlated with conductivity (Table 3).

The univariate model of conductivity was identified as the best model to predict macroinvertebrate occurrence because it was the only environmental predictor significantly ($p < .05$) correlated with this response variable (Table 3, Figure 2). The best model for predicting Isotomidae abundance was a two-variable model consisting of conductivity and mean ice to water surface depth (Table 4), which highlighted the negative correlation of conductivity and positive correlation of mean ice to water surface depth with Isotomidae abundance (Figure 2). The best Isotomidae abundance model had the lowest absolute AICc value and the greatest *Wi* value from among all models (Table 4, Table S2). Five models (Water temperature + Conductivity + Ice to water surface depth; Conductivity + Number of supraglacial pools within 5 m; Water temperature + Conductivity + Number of supraglacial pools within 5 m; Conductivity + Ice to water surface depth + Number of supraglacial pools within 5 m; Conductivity + Ice to water surface depth + Ablation zone) exhibited AICc values within 2 AICc units of the best Isotomidae abundance model (Table 4, Table S2), which indicates that there is substantial support for these five models based on the AICc values (Burnham and Anderson 2002). However, the *Wi* values for these five models exhibited between 33 and 61 percent difference from the best Isotomidae abundance model (Table 4, Table S2), which supports our identification of the Conductivity + Ice to water surface model as the best Isotomidae abundance model. We did note that the best Isotomidae abundance model did not have the greatest percentage deviance values (Table 4, Table S2). However, percentage deviance values increased with number of environmental predictors in a model (i.e., *k*; Table S2), which suggests that percentage deviance values should only be compared among models with the same number of environmental predictors. The best Isotomidae abundance model exhibited the greatest percentage deviance from among all two variable models and it was similar (±2 percent) in percentage deviance to the second best Isotomidae abundance model with three variables (water temperature, conductivity, and ice to water surface depth; Table 4, Table S2).

The best model predicting macroinvertebrate abundance in supraglacial pools was a two-variable model with conductivity and number of supraglacial pools within 5 m (Table 4) that documented the negative correlation of conductivity and positive relationship between number of supraglacial pools within 5 m and macroinvertebrate abundance (Figure 2). The best macroinvertebrate abundance model was less than 2 AIC units from a three-factor model with Conductivity + Number of supraglacial pools within 5 m + Ice to water surface depth (Table 4). However, the *Wi* value for the three-factor model was 58 percent different from the best macroinvertebrate abundance model, which supports our identification of the two-factor model with Conductivity + Number of supraglacial pools within 5 m as the best model. The best two-factor model for macroinvertebrate abundance did not have the greatest percentage deviance, which again supports using this metric only for comparing models with the same number of environmental predictors.

Two models for Isotomidae occurrence (Conductivity and Conductivity + Mean water depth) were within two AICc units of each other, with the two-factor model having the lowest AICc value (Table 4). The *Wi* value for the two-factor model was only 11 percent higher than that for the univariate model with conductivity. However,

Table 3. Generalized linear model analysis results of the relationships of macroinvertebrate response variables with thirteen physical, chemical, and glacier landscape variables within supraglacial pools on the Hailuogou Glacier, Ganze Tibetan Autonomous Region, China, June 2018 and August 2019.

Response variable	Independent variable(s)	Estimate	*p*
Chironomidae abundance	Water temperature, pH, conductivity, turbidity, mean water depth, surface area, mean ice to water surface depth, distance from north to south boundary, distance to closest pool, number of pools within 5 m, ablation zone, substrate richness, mean grain size	—	>.070
Isotomidae abundance	Water temperature	−1.359	.019
Isotomidae abundance	Conductivity	−120.566	<.001
Isotomidae abundance	Mean ice to water surface depth	3.899	.006
Isotomidae abundance	Number of holes within 5 m	1.122	.009
Isotomidae abundance	Ablation zone	−1.337	.042
Isotomidae abundance	pH, turbidity, mean water depth, surface area, distance from north to south boundary, distance of closest pool, substrate richness, mean grain size	—	>.120
Macroinvertebrate abundance	Conductivity	−99.195	<.001
Macroinvertebrate abundance	Mean ice to water surface depth	3.002	.005
Macroinvertebrate abundance	Number of holes within 5 m	1.041	<.001
Macroinvertebrate abundance	Water temperature, pH, turbidity, mean water depth, surface area, distance from north and south boundaries, distance of closest pool, ablation zone, substrate richness, mean grain size	—	>.110
Chironomidae occurrence	Water temperature, pH, conductivity, turbidity, mean water depth, surface area, mean ice to water surface depth, distance from north to south boundary, distance to closest pool, number of pools within 5 m, ablation zone, substrate richness, mean grain size	—	>.050
Isotomidae occurrence	Conductivity	−156.190	.002
Isotomidae occurrence	Mean water depth	2.042	.046
Isotomidae occurrence	Water temperature, pH, turbidity, surface area, mean ice to water surface depth, distance from north and south boundaries, distance of closest pool, number of pools within 5 m, ablation zone, substrate richness, mean grain size	—	>.090
Macroinvertebrate occurrence	Conductivity	−151.293	.002
Macroinvertebrate occurrence	Water temperature, pH, turbidity, mean water depth, surface area, mean ice to water surface depth, distance from north and south boundaries, distance of closest pool, number of pools within 5 m, ablation zone, substrate richness, mean grain size	—	>.280

Note. Environmental variables that had a significant effect ($p < .05$) were used within our multimodel inference analyses. Details from the results of environmental variables with nonsignificant results ($p < .05$) are provided in the Supplementary Material Table S1.

within the two-variable model only conductivity had a significant effect ($p < .05$) on Isotomidae occurrence. Therefore, we selected the univariate model documenting a negative relationship between Isotomidae occurrence and conductivity as the best model to predict Isotomidae occurrence (Figure 2).

Discussion

Comparison of physical and chemical characteristics between supraglacial pools and cryoconite holes

One of the most interesting differences between the supraglacial pools of a debris-covered glacier and cryoconite holes from other regions is the greater diversity of supraglacial pool shapes, sizes, water depths, and ice to water surface depths found on the Hailuogou Glacier. Cryoconite holes are cylindrical (Porazinska et al. 2004), near-vertical tubes (Tranter et al. 2004), D-shaped on north-facing slopes, and elongated after sediment-driven dynamics merge multiple cylindrical holes (Cook et al. 2018). Cryoconite holes have been noted with shallow profiles and indistinct edge boundaries on the Greenland Ice Sheet (Zawierucha et al. 2018). Supraglacial pools on the Hailugou Glacier exhibited all of the described cryoconite hole shapes as well as ovoid, rectangular, and irregular polygon shapes (Figure 3). The shape of supraglacial pools on debris-covered glaciers may be a result of many factors, including the stippled surface of the glacier (e.g., small crevasses), differential heating due to topography shading effects, diurnal melt patterns causing frequent movement of debris into the pools, and large debris on the glacier surface near the pools. Thermal characteristics of debris and the movement of the debris into pools could be elongating the shape of pools such as those seen on the Hailuogou Glacier at the base of small crevasses (Figure 3). In addition, as a temperate glacier, melt patterns may be created that allow meltwater pools to expand deep within the glacier during the ablation season.

The mean LW of supraglacial pools on the Hailuogou Glacier was greater than the mean diameters of cryoconite holes in Greenland, Canada, Italy, Nepal, Antarctica, and King George Island (Table 1). Additionally, the maximum LW from Hailuogou Glacier (228 cm) was greater than the maximum diameter of cryoconite holes on the Greenland Ice Cap (>100 cm; Gerdel and Drouet 1960). This difference may be due to a tendency for studies to focus on higher elevation areas where cryoconite is located and not on the ablation zones close to the glacier or ice sheet termini. Cook

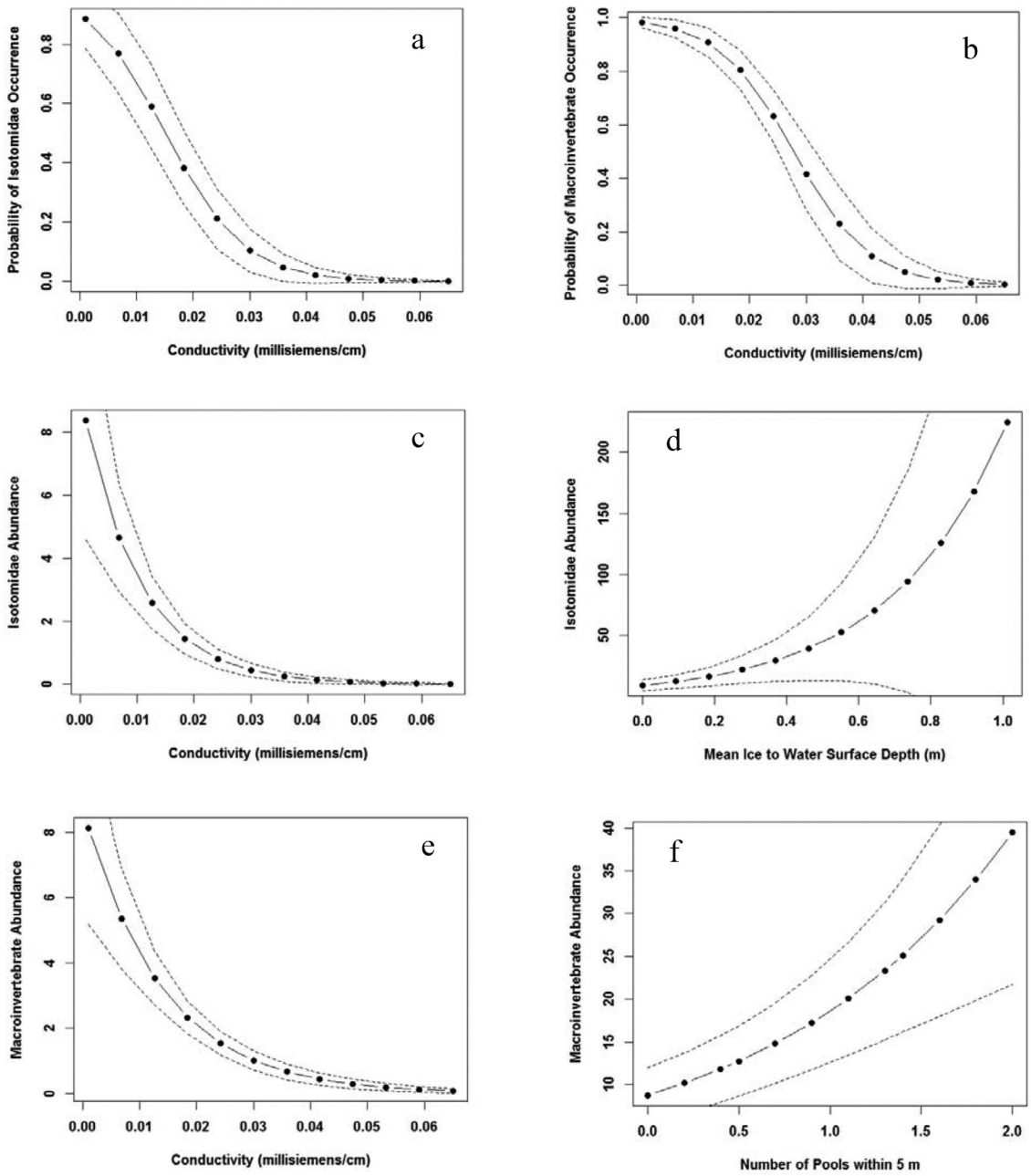

Figure 2. Predicted relationships between (a) Isotomidae occurrence and conductivity, (b) macroinvertebrate occurrence and conductivity, (c) Isotomidae abundance and conductivity, (d) Isotomidae abundance and mean ice to water surface depth, (e) macroinvertebrate abundance and conductivity, and (f) macroinvertebrate abundance and number of supraglacial pools within 5 m within supraglacial pools on the Hailuogou Glacier, Ganze Tibetan Autonomous Region, China, June 2018 and August 2019.

et al. (2010) noted decreasing sizes of cryoconite holes with increasing elevation on the Greenland Ice Sheet. Understanding how the sizes of cryoconite holes and supraglacial pools vary with distance from the glacier termini would confirm whether there is a gradient of meltwater habitat sizes on glaciers and ice sheets. Our findings suggest that the frequency of supraglacial pools with mean LW less than 5 cm is very low on the Hailuogou Glacier. Additionally, the mean surface area of Hailuogou Glacier supraglacial pools was between 2.1 to 5.5 times larger than the surface area of the cryoconite holes on Svalbard, Canada, and Antarctica (Table 1). The maximum surface area we observed (45,725 cm^2) was greater than the maximum surface areas found in Greenland and Antarctica (Table 1). The greater sizes we observed in supraglacial pools might be a function of our focus on sampling pools likely to hold macroinvertebrates. A more comprehensive study of the size frequency distribution of supraglacial pools on debris-covered glaciers throughout the ablation season is needed.

Table 4. Summary of the number of parameters (*k*), small sample Akaike information criterion (AICc), difference in AICc between each model and the model with the minimum AICc (ΔAICc), Akaike weight (*Wi*), and percentage deviance (%Dev) from the three best models of the generalized linear model analyses of Isotomidae abundance, macroinvertebrate abundance, Isotomidae occurrence selected environmental predictors within supraglacial pools on the Hailuogou Glacier, Ganze Tibetan Autonomous Region, China, June 2018 and August 2019.

Response variable	Independent variable	*k*	AICc	ΔAICc	*Wi*	%Dev
Isotomidae abundance	C, IWSD	2	189.32	0.00	0.18	43.01
Isotomidae abundance	WT, C, IWSD	3	190.18	0.86	0.12	45.29
Isotomidae abundance	C, NP5M	2	190.56	1.25	0.10	41.07
Macroinvertebrate abundance	C, NP5M	2	216.70	0.00	0.62	50.70
Macroinvertebrate abundance	C, NP5M, IWSD	3	218.45	1.75	0.26	51.78
Macroinvertebrate abundance	C, IWSD	2	220.51	3.81	0.09	0.00
Isotomidae occurrence	C, MWD	2	48.08	0.00	0.53	34.91
Isotomidae occurrence	C	1	48.32	0.24	0.47	30.93
Isotomidae occurrence	MWD	1	61.61	13.53	0.00	10.09

Notes. Additional details from the results of twenty-four additional Isotomidae abundance models and four macroinvertebrate abundance models are available in the Supplementary Materials Table S2. C = conductivity; IWSD = mean ice to water surface depth; WT = water temperature; NH5M = number of pools within 5 m; MWD = mean water depth.

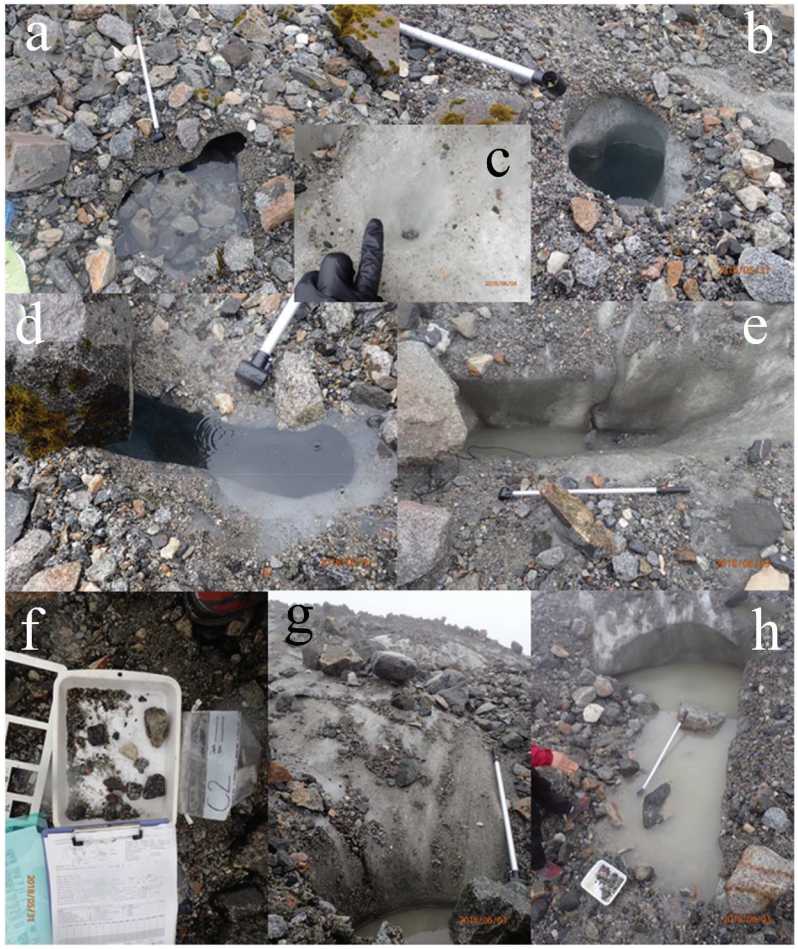

Figure 3. Photographs of Hailuogou Glacier supraglacial pools that depict the various shapes and different ice surface–to–water depths observed. Some supraglacial pools had (a), (d) water located at the surface of the ice and others had (b), (e) water levels below the surface of the glacier ice. (c) The genesis of a pool was captured in the upper zone of the ablation tongue. (f) Typical sediment sampled in a supraglacial pool, (g) sediment precipitously positioned on ice above a pool, and (h) the formation of a pool at the base of a small crevasse. The velocity meter in the images is 1.14 m long.

Comparisons of supraglacial meltwater habitats on the accumulation zone and ablation zones of the same glaciers/ice sheets are needed to understand the dynamics of the formation of supraglacial pools and cryoconite holes at different elevations. We observed one small depression with sand substrate that appeared

to be the beginning stages of a supraglacial pool on the upper ablation zone underneath a boulder on an ice mound (Figure 3). Documenting the genesis of debris-covered supraglacial pools would add to our understanding of how elevation and location influences the formation of these glacial meltwater habitats and may give insights into factors influencing biotic community development.

Mean supraglacial pool water depth and maximum water depths on the Hailuogou Glacier were greater than the mean and maximum water depths from cryoconite holes in Svalbard, Greenland, Canada, Nepal, and Antarctica (Table 1). The greater mean water depths in Hailuogou Glacier supraglacial pools could be due to the polythermal nature of the temperate monsoonal glacier ice, pool age, or the movement of the glacier extending the pools deeper within the glacier. However, until the genesis and development of supraglacial pools on debris-covered glaciers are quantified, these and other mechanisms including biotic ones cannot be ruled out as influential in their formation.

The sediment in the Hailuogou Glacier supraglacial pools consists of a heterogeneous mixture of loose, inorganic sediment ranging from fine silt (<1 mm) to large boulders (>256 mm). The difference in sediment types and sizes we observed in Hailuogou Glacier supraglacial pools could be due to a combination of the available sediment sources including ice falls, debris flows, and supraglacial substrate movement from steep gradient ice on the glacier surface (Figure 3). Cryoconite is essentially sand covered with layers of periphyton and heterotrophic microorganisms (Takeuchi et al. 2000; Mueller et al. 2001; Tranter et al. 2004; Hodson et al. 2008), so a comparison of periphyton and heterotrophic microorganisms on larger substrate from supraglacial pools with that on cryoconite would enhance the understanding of ecological differences between supraglacial habitat types and primary productivity. We did not observe the accumulation of autotrophic and heterotrophic microorganisms wrapped around sand grains in Hailuogou Glacier supraglacial pools. Occasionally, we observed periphyton and/or moss growing on cobble and boulder substrates in shallow supraglacial pools. The difference between cryoconite substrate and supraglacial pool substrate sizes may create ecological conditions on debris-covered glaciers that attract colonization of macroinvertebrates.

The mean pH values observed in Hailuogou Glacier supraglacial pools were neutral and fell within the range of mean pH values from cryoconite holes in Svalbard, Greenland, Canada, and Antarctica (Table 1). Mean conductivity from Hailuogou Glacier supraglacial pools fell within the range of observed conductivity values from cryoconite holes in Svalbard, Canada, Italy, and Antarctica (Table 1). The range of water temperatures (−0.01°C to 4.5°C) we observed from Hailuogou Glacier supraglacial pools from late May to early August of 2018 and 2019 encompassed warmer water temperatures than the range of water temperatures from cryoconite holes in Svalbard, Canada, and Antarctica, which did not exceed 2.0°C (Table 1). However, only three of the forty-six Hailuogou Glacier supraglacial pools had water temperatures higher than 2°C (3°C–4.5°C). These three supraglacial pools had lower mean water depths (6.7 cm) than the other forty-three supraglacial pools that had water temperatures lower than 2.0°C and greater mean water depths (39.2 cm). These shallow pools also contained gravel and sand substrate, which may have played in the role of increasing the water temperature. However, comparisons of our observed water temperatures with others are likely confounded by different climatic conditions in the temperate monsoon region compared to polar, temperate, and other climate regimes where cryoconite hole studies were performed. Future research controlling for temporal variation in water temperature is needed to determine the influence of debris and the monsoon climate on water temperatures in supraglacial pools.

Comparison of macroinvertebrate fauna and habitat relationships between supraglacial pools and cryoconite holes

Natural history surveys of cryoconite holes documented the meiofauna (<500 μm in size) taxa Rotifera, Tardigrada, and Copepoda and the macroinvertebrate (>500 μm in size) taxa Chironomidae within cryoconite holes on glaciers in Asia (Zawierucha et al. 2015). Our documentation of Chironomidae from Hailuogou Glacier cryoconite holes is consistent with these findings from Asia. Chironomidae are common macroinvertebrates found in glacier stream sites located within in the metakryal zone of the Hailuogou Glacier (Fair 2017), and their occurrence in Hailuogou Glacier supraglacial pools was anticipated. Our results also represent the first documentation of Collembola from meltwater habitats (i.e., cryoconite holes and supraglacial pools) on glaciers in Asia. Previously, Collembola have been documented from cryoconite holes on the Tyndall Glacier in Patagonia, Chile (Takeuchi and Kohshima 2004; Zawierucha et al. 2015), the Forni Glacier in Italy (Zawierucha, Buda, Azzoni et al. 2019), and the Adishi Glacier in Georgia (Makowska et al. 2016). Additionally, Collembola were found within meltwater ponds in Alaska and British Columbia (Fjellberg 2010). Our sampling method was designed to capture macroinvertebrates, not the meiofauna taxa that have been documented in Asian

cryoconite holes (Zawierucha et al. 2015). Future research in supraglacial pools in Tibet needs to use sampling methods capable of capturing meiofauna to determine whether they are a constituent of the supraglacial pool communities.

We quantified that Isotomidae occurrence, Isotomidae abundance, macroinvertebrate abundance, and macroinvertebrate occurrence were correlated with water chemistry variables (i.e., water temperature, conductivity), physical habitat variables (mean water depth, mean ice-to–surface water depth), and glacier environmental variables (ablation zone, number of supraglacial pools within 5 m). Studies evaluating the habitat relationships of the meiofauna taxa documented that Tardigrada density, Tardigrada occurrence, and Rotifera density were correlated with water chemistry variables (pH, nutrient concentrations), physical habitat variables (cryoconite hole diameter), and climatic variables (storm events) in cryoconite holes in Svalbard and Antarctica (Porazinska et al. 2004; Vonnahme et al. 2016; Zawierucha, Ostrowska et al. 2016; Zawierucha, Buda, and Nawrot 2019). Our results represent the first documentation of the importance of conductivity for the occurrence and abundance of macroinvertebrates in supraglacial pools. We suspect that conductivity may be serving as an indicator of supraglacial pool nutrient concentrations and future research needs to evaluate the relationships of macroinvertebrates with nutrient concentrations. Our results and those from Svalbard and Antarctica (Porazinska et al. 2004; Vonnahme et al. 2016; Zawierucha, Ostrowska et al. 2016) suggest the importance of water chemistry variables and physical habitat variables for the meiofauna and macroinvertebrate communities in cryoconite holes and supraglacial pools.

We were surprised that none of the selected water chemistry, physical habitat, and glacier environmental variables had a significant relationship with Chironomidae abundance and occurrence. We had expected to observe relationships of Chironomidae with water temperature because of the well-known affinity of cryophilic Diamesinae chironomids with near-freezing water temperature and the close distance of the glacier to glacial melt streams (Milner 2016). We also thought the Hailuogou Glacier streams would serve as a potential source of Chironomidae for supraglacial pools because Chironomidae are common within stream communities located near the snout of the Hailuogou Glacier (Fair 2017). Rotifera and Tardigrada exhibited relationships with environmental variables in several studies (Porazinska et al. 2004; Vonnahme et al. 2016; Zawierucha, Ostrowska et al. 2016), but studies in Svalbard and Greenland documented that Rotifera and Tardigrada abundances were not correlated with water depth, pH, nutrient concentrations, or elevation (Zawierucha, Vonnahme et al. 2016; Zawierucha et al. 2018; Zawierucha, Buda, and Nawrot 2019). The lack of significant environmental relationships in these studies was attributed to the cryoconite holes being unstable as a result of lacking an ice cap, melting conditions, and flushing events from storms. Perhaps our observation of Chironomidae not exhibiting significant correlations with any measured environmental variable reflects the unstable nature of Hailuogou Glacier supraglacial pools. Alternatively, perhaps adult Chironomidae randomly selected supraglacial pools to deposit eggs or responded to an unmeasured environmental variable. Moreover, the timing of our sampling may have corresponded with a postemergence period for Chironomidae and the low number of Chironomidae larvae observed were the late emergers that remained. Future research needs to evaluate whether Chironomidae habitat relationships in supraglacial pools fluctuate seasonally as a result of storm events, insect emergence cycles, and/or availability of periphyton food resources.

We also identified that the best models to predict the abundance and occurrence of Isotomidae and macroinvertebrates all contained conductivity either in a univariate model or in a two-variable multivariate model along with either a physical habitat variable (mean ice to water surface depth) or a glacier landscape variable (number of supraglacial pools within 5 m). These results highlight the need for future research to identify the causal mechanisms underlying the relationships between the abundance and occurrence of Isotomidae and macroinvertebrates with conductivity in supraglacial pools. Notably, the relationship of Isotomidae with conductivity and mean ice to water surface depth was unexpected. Isotomidae are semi-aquatic macroinvertebrates found in a range of glacier habitat types from glacial ice fields to meltwater pools to glacier streams (Fjellberg 2010). Collembola within glacial meltwater habitats have been observed on the water surface and underwater on the benthic sediment (Takeuchi and Kohshima 2004; Zawierucha, Buda, Azzoni et al. 2019). Semi-aquatic Collembola typically live on the water surface and on vegetation at the edges of aquatic habitats, but some species have been documented to survive up to forty days underwater (Deharveng, D'Haese, and Bedos 2008). However, little is known about the habitat relationships of Collembola in glacial meltwater habitats. Isotomidae and other Collembola possess a collophore with an eversible vesicle that absorbs water, chloride, sodium, potassium, and hydrogen and excretes ammonia (Eisenbeis 1982; Konopová, Kolosov, and O'Donnell 2019). Perhaps this osmoregulatory appendage combined with its surface-dwelling habit explains why Isotomidae abundance was able to increase with decreasing

conductivity levels. The association of Isotomidae with increasing ice to water surface depth may be due to increasing protection from the wind and other climatic variables. Additionally, the supraglacial pools with large ice to water surface depths may have functioned like pitfall traps for Isotomidae originating from areas adjacent to the pools. We recommend that future research quantify Collembola microhabitat use and explore how their microhabitat preferences influence their responses to environmental variables in glacial meltwater habitats.

Conclusions

Supraglacial pools on a debris-covered glacier in southeast Tibet have a wide range of shapes, are larger and deeper, and contain a greater diversity of substrate sizes than cryoconite holes from polar regions and colder glaciers in High Mountain Asia. We also found that the studied supraglacial pools frequently contained two macroinvertebrate taxa that do not occur regularly in cryoconite holes on clean glaciers from other parts of the world. Additionally, our results highlighted the novel relationships of the abundance and occurrence of these two macroinvertebrate taxa with conductivity within supraglacial pools of this debris-covered glacier. Our results also highlight that supraglacial pools on a debris-covered glacier in southeast Tibet are unique physically, chemically, and biologically compared to cryoconite holes from other parts of the world. Future research needs to quantitatively compare the differences between supraglacial pools on debris-covered glaciers and those on clean glaciers in the region and around the world to increase our understanding of these unique ecosystems that are threatened by climate change.

Acknowledgments

We thank Earl Greene (United States Geological Survey), Wang Genxu, Liu Faming, and Lan Quan (Chinese Academy of Sciences Institute for Mountain Hazards and Environment) for their support and assistance with fieldwork. We also thank the anonymous reviewers for their suggestions that improved the article.

Disclosure statement

No potential conflicts of interest were reported by the authors.

Funding

This study was funded by the Columbus Zoo Biodiversity Conservation Fund and the National Natural Science Foundation of China (NSFC 41871069).

ORCID

Heather Fair http://orcid.org/0000-0002-1085-0311
Peter C. Smiley Jr. http://orcid.org/0000-0002-8772-4102
Liu Qiao http://orcid.org/0000-0002-7285-5425

References

Adams, W. P. 1966. Studies of ablation and run-off on an Arctic glacier. Doctoral diss., McGill University, Montreal, Canada.

Bagshaw, E. A., M. Tranter, J. L. Wadham, A. G. Fountain, and M. Mowlem. 2011. High-resolution monitoring reveals dissolved oxygen dynamics in an Antarctic cryoconite hole. *Hydrological Processes* 25 (18):2868–77. doi:10.1002/hyp.8049.

Baker, B. B., and R. K. Moseley. 2007. Advancing treeline and retreating glaciers: Implications for conservation in Yunnan, P.R. China. *Arctic, Antarctic, and Alpine Research* 39 (2):200–09. doi:10.1657/1523-0430(2007)39[200:atargi]2.0.co;2.

Buda, J., E. Łokas, M. Pietryka, D. Richter, W. Magowski, N. S. Iakovenko, D. L. Porazinska, T. Budzik, M. Grabiec, J. Grzesiak, et al. 2020. Biotope and biocenosis of cryoconite hole ecosystems on ecology glacier in the maritime Antarctic. *Science of the Total Environment* 274. doi:10.1016/j.scitotenv.2020.138112.

Burnham, K. P., and D. R. Anderson. 2002. *Model selection and multimodel inference: A practical information-theoretic approach*. New York: Springer.

Caccianiga, C., C. Andreis, G. Diolaiuti, C. D'Agata, C. Mihalcea, and C. Smiraglia. 2011. Alpine debris-covered glaciers as a habitat for plant life. *The Holocene* 21:1011–20. doi:10.1177/0959683611400219.

Cook, J. M., I. Hodson, J. Telling, A. Anesio, T. Irvine-Fynn, and C. Bellas. 2010. The mass–area relationship within cryoconite holes and its implications for primary production. *Annals of Glaciology* 51:106–10. doi:10.3189/172756411795932038.

Cook, J. M., M. Sweet, O. Cavalli, A. Taggart, and A. Edwards. 2018. Topographic shading influences cryoconite morphodynamics and carbon exchange. *Arctic, Antarctic, and Alpine Research* 50:1. doi:10.1080/15230430.2017.1414463.

Darcy, J. L., E. M. S. Gendron, P. Sommers, D. L. Porazinska, and S. K. Schmidt. 2018. Island biogeography of cryoconite hole bacteria in Antarctica's Taylor Valley and around the world. *Frontiers in Ecology and Evolution* 6:180. doi:10.3389/fevo.2018.00180.

De Smet, W. H., and E. A. Van Rompu. 1994. Rotifera and Tardigrada from some cryoconite holes on a Spitsbergen Svalbard glacier. *Belgian Journal of Zoology* 124:27–37.

Deharveng, L., C. A. D'Haese, and A. Bedos. 2008. Global diversity of springtails (Collembola; Hexapoda) in freshwater. *Hydrobiologia* 595:329–38. doi:10.1007/s10750-007-9116-z.

Edwards, A., A. Anesio, S. M. Rassner, B. Sattler, B. Hubbard, W. T. Perkins, M. Young, and G. W. Griffith. 2011. Possible interactions between bacterial diversity, microbial activity and supraglacial hydrology of cryoconite holes in Svalbard. *The ISME Journal* 5:150–60. doi:10.1038/ismej.2010.100.

Eisenbeis, G. 1982. Physiological absorption of liquid water by Collembola: Absorption by the ventral tube at different

salinities. *Journal of Insect Physiology* 28:11–20. doi:10.1016/0022-1910(82)90017-8.
ESRI. 2013. *Arc map version 10.2*. Redlands, CA: ESRI Inc.
Fair, H. 2017. Ecology of aquatic insects in monsoonal temperate glacier streams of Southeast Tibet: A departure from the conceptual model. Doctoral diss., The Ohio State University, Columbus.
Fjellberg, A. 2010. Cryophilic Isotomidae (Collembola) of the Northwestern Rocky Mountains, U. S. A. *Zootaxa* 2513:27–79. doi:10.5281/zenodo.196078.
Fujii, Y., and K. Higuchi. 1977. Statistical analyses of the forms of the glaciers in the Khumbu Himal. *Journal of Japanese Society of Snow and Ice* 39:7–14. doi:10.5331/seppyo.39.special_7.
Fyffe, C. L., B. W. Brocka, M. P. Kirkbrideb, D. W. F. Mairc, N. S. Arnold, C. Smiragliae, G. Diolaiutie, and F. Diotrif. 2019. Do debris-covered glaciers demonstrate distinctive hydrological behavior compared to clean glaciers? *Journal of Hydrology* 570:584–97. doi:10.1016/j.jhydrol.2018.12.069.
Gerdel, R. W., and F. Drouet. 1960. The cryoconite of the Thule Area, Greenland. *Transactions of the American Microscopical Society* 79:256–72. doi:10.2307/3223732.
Guisan, A., and N. E. Zimmermann. 2000. Predictive habitat distribution models in ecology. *Ecological Modelling* 135:147–86. doi:10.1016/S0304-3800(00)00354-9.
He, Y. Q., Z. X. Li, X. M. Yang, W. X. Jia, X. Z. He, B. Song, N. N. Zhang, and Q. Liu. 2008. Changes of the Hailuogou Glacier, Mt. Gongga, China, against the background of global warming in the last several decades. *Journal of China University of Geosciences* 19:271–81. doi:10.1016/S1002-0705(08)60045-X.
Hodson, A., A. M. Anesio, M. Tranter, A. Fountain, M. Osborn, J. Priscu, J. Laybourn-Parry, and B. Sattler. 2008. Glacial ecosystems. *Ecological Monographs* 78:41–67. doi:10.1890/07-0187.1.
Johnson, J. B., and K. S. Omland. 2004. Model selection in ecology and evolution. *Trends in Ecology and Evolution* 19:101–08. doi:10.1016/j.tree.2003.10.013.
Konopová, B., D. Kolosov, and M. J. O'Donnell. 2019. Water and ion transport across the eversible vesicles in the collophore of the springtail *Orchesella cincta*. *Journal of Experimental Biology* 34:261–66. doi:10.1242/jeb.200691.
Liu, Q., and S. Liu. 2010. Seasonal evolution of the englacial and subglacial drainage systems of a temperate glacier revealed by hydrological analysis. *Sciences in Cold and Arid Regions* 21:51–58.
Liu, Q., S. Y. Liu, Y. Zhang, X. Wang, Y. Zhang, W. Guo, and J. Xu. 2010. Recent shrinkage and hydrological response of Hailuogou glacier, a monsoon temperate glacier on the east slope of Mount Gongga, China. *Journal of Glaciology* 56:215–24. doi:10.3189/002214310791968520.
Makowska, N., K. Zawierucha, J. Mokracka, and R. Koczura. 2016. First report of microorganisms of Caucasus glaciers (Georgia). *Biologia* 71:620–25. doi:10.1515/biolog-2016-0086.
Margesin, R., and V. Miteva. 2011. Diversity and ecology of psychrophilic microorganisms. *Research in Microbiology* 162:346–61. doi:10.1016/j.resmic.2010.12.004.
Mazerolle, M. J. 2020. AICcmodavg: Model selection and multimodel inference based on (Q)AIC(c). *R package version 2.3-1*. https://cran.r-project.org/package=AICcmodavg.
McIntyre, N. F. 1984. Cryoconite hole thermodynamics. *Canadian Journal of Earth Sciences* 21:152–56. doi:10.1139/e84-016.
Merritt, R. W., K. W. Cummins, and M. B. Berg. 2008. *An introduction to the aquatic insects of North America*. 4th ed. Dubuque, IA: Kendall Hunt Publishers.
Milner, A. M. 2016. The Milner and Petts (1994) conceptual model of community structure within glacier-fed rivers: 20 years on. In *River science: Research and management for the 21st century*, ed. D. J. Gilvear, M. T. Greenwood, M. C. Thoms, and P. J. Wood, 156–70. West Sussex, UK: Wiley and Sons.
Mueller, D. R., W. F. Vincent, W. H. Pollard, and C. H. Fristen. 2001. Glacial cryoconite ecosystems: A bipolar comparison of algal communities and habitats. *Nova Hedwig Beih* 123:173–97.
Pittino, F., M. Maglio, I. Gandolfi, and R. S. Azzoni. 2018. Bacterial communities of cryoconite holes of a temperate alpine glacier show both seasonal trends and year-to-year variability. *Annals of Glaciology* 59:1–9. doi:10.1017/aog.2018.16.
Porazinska, D. L., A. G. Fountain, T. H. Nylen, M. Tranter, R. A. Virginia, and D. H. Wall. 2004. The biodiversity and biogeochemistry of cryoconite holes from McMurdo Dry Valley Glaciers, Antarctica. *Arctic, Antarctic, and Alpine Research* 36:84–91. doi:10.1657/1523-0430(2004)036[0084:tbaboc]2.0.co;2.
R Core Team. 2017. *R version 3.3.3: A language and environment for statistical computing*. R Vienna, Austria: Foundation for Statistical Computing, Vienna.
Sommers, P., J. L. Darcy, E. M. S. Gendron, L. F. Stanish, E. A. Bagshaw, D. L. Porazinska, and S. K. Schmidt. 2018. Diversity patterns of microbial eukaryotes mirror those of bacteria in Antarctic cryoconite holes. *FEMS Microbial Ecology* 94:1–11. doi:10.1093/femsec/fix167.
Takeuchi, N., and S. Kohshima. 2004. A snow algal community on Tyndall Glacier in the Southern Patagonia Icefield, Chile. *Arctic, Antarctic, and Alpine Research* 36:92–99. doi:10.1657/1523-0430(2004)036[0092:asacot]2.0.co;2.
Takeuchi, N., S. Kohshima, Y. Yoshimura, K. Setko, and K. Fujita. 2000. Characteristics of cryoconite holes on a Himalayan glacier, Yala Glacier Central Nepal. *Bulletin of Glaciological Research* 17:51–59.
Takeuchi, N., R. Sakaki, J. Uetake, N. Nagatsuka, R. Shimada, M. Niwano, and T. Aoki. 2018. Temporal variations of cryoconite holes and cryoconite coverage on the ablation ice surface of Qaanaaq Glacier in northwest Greenland. *Annals of Glaciology* 59:21–30. doi:10.1017/aog.2018.19.
Telling, J., A. M. Anesio, M. Tranter, A. G. Fountain, T. Nylen, J. Hawkings, V. B. Singh, P. Kaur, M. Musilova, and J. L. Wadham. 2014. Spring thaw ionic pulses boost nutrient availability and microbial growth in entombed Antarctic Dry Valley cryoconite holes. *Frontiers in Microbiology* 5:694. doi:10.3389/fmicb.2014.00694.
Tranter, M., A. G. Fountain, C. H. Fritsen, W. B. Lyons, J. C. Priscu, P. J. Statham, and K. A. Welch. 2004. Extreme hydrochemical conditions in natural microcosms entombed within Antarctic ice. *Hydrological Processes* 18 (2):379–87. doi:10.1002/hyp.5217.
Venables, W. N., and B. D. Ripley. 2002. *Modern applied statistics with S*. New York: Springer Science+Business Media.

Vonnahme, T. R., M. Devetter, J. D. Žarský, M. Šabacká, and J. Elster. 2016. Controls on microalgal community structures in cryoconite holes upon High Arctic glaciers, Svalbard. *Biogeosciences* 12:11751–95. doi:10.5194/bg-13-659-2016.

Wharton, R. A., C. P. McKay, G. M. Simmons Jr., and B. C. Parker. 1985. Cryoconite holes on glaciers. *BioScience* 35:499–503. doi:10.2307/1309818.

Yao, T. D., L. Thompson, W. Yang, W. S. Yu, Y. Gao, X. J. Guo, X. X. Yang, K. Q. Duan, H. B. Zhao, B. Q. Xu, et al. 2012. Different glacier status with atmospheric circulations in Tibetan Plateau and surroundings. *Nature Climate Change* 2:663–67. doi:10.1038/nclimate1580.

Zawierucha, K., J. Buda, R. S. Azzoni, M. Niskiewicz, A. Franzetti, and R. Ambrosini. 2019. Water bears dominated cryoconite hole ecosystems: Densities, habitat preferences and physiological adaptations of Tardigrada on an alpine glacier. *Aquatic Ecology* 53:543–56. doi:10.1007/s10452-019-09707-2.

Zawierucha, K., J. Buda, D. Fontaneto, R. Abrosini, A. Franzetti, M. Wierzgon, and M. Bogdziewicz. 2019. Fine-scale spatial heterogeneity of invertebrates within cryoconite holes. *Aquatic Ecology* 53:179–90. doi:10.1007/s10452-019-09681-9.

Zawierucha, K., J. Buda, and A. Nawrot. 2019. Extreme weather events results in the removal of invertebrates from cryoconite holes on an Arctic valley glacier (Longyearbreen, Svalbard). *Ecological Research* 34:370–79. doi:10.1111/1440-1703.1276.

Zawierucha, K., J. Buda, M. Pietryka, M. Pietryka, D. Richter, E. Lokas, S. Lehmann-Konera, N. Makowska, and M. Bogdziewicz. 2018. Snapshot of micro-animals and associated biotic and abiotic environmental variables on the edge of the south-west Greenland ice sheet. *Limnology* 19:141–50. doi:10.1007/s10201-017-0528-9.

Zawierucha, K., M. Kolicka, N. Takeuchi, and L. Kaczmarek. 2015. What animals can live in cryoconite holes? A faunal review. *Journal of Zoology* 295:159–69. doi:10.1111/jzo.1219.

Zawierucha, K., M. Ostrowska, T. R. Vonnahme, M. Devetter, A. P. Nawrot, S. Lehman, and M. Kolicka. 2016. Diversity and distribution of Tardigrada in Arctic cryoconite holes. *Journal of Limnology* 75:545–59.

Zawierucha, K., T. R. Vonnahme, M. Devetter, M. Kolicka, M. Ostrowska, S. Chmielewski, and J. Z. Kosicki. 2016. Area, depth and elevation of cryoconite holes in the Arctic do not influence Tardigrada densities. *Polish Polar Research* 37:325–34. doi:10.1515/popore-2016-0009.

Zhang, Y., K. Fujita, S. Y. Liu, Q. Liu, and N. Takayuki. 2011. Distribution of debris thickness and its effect on ice melt at Hailuogou glacier, southeastern Tibetan Plateau, using in situ surveys and ASTER imagery. *Journal of Glaciology* 571147–57. doi:10.3189/002214311798843331.